The Journal of Infectious Diseases

MAJOR ARTICLE

Role of Purine Biosynthesis in Persistent Methicillin-Resistant *Staphylococcus aureus* Infection

Liang Li,[1] Wessam Abdelhady,[1] Niles P. Donegan,[3] Kati Seidl,[4] Ambrose Cheung,[3] Yu-Feng Zhou,[1,5] Michael R. Yeaman,[1,2] Arnold S. Bayer,[1,2] and Yan Q. Xiong[1,2]

[1]Los Angeles Biomedical Research Institute, Harbor-UCLA Medical Center, Torrance, and [2]David Geffen School of Medicine at UCLA, Los Angeles, California; [3]Dartmouth Medical School, Hanover, New Hampshire; [4]University Hospital of Zurich, Switzerland; and [5]South China Agricultural University, Guangzhou

Persistent methicillin-resistant *Staphylococcus aureus* (MRSA) bacteremia (PB) represents an important subset of *S. aureus* endovascular infections. In this study, we investigated potential genetic mechanisms underlying the persistent outcomes. Compared with resolving bacteremia (RB) isolates (defined as isolates associated with negative results of blood cultures 2–4 days after initiation of therapy), PB strains (defined as isolates associated with positive results of blood cultures ≥7 days after initiation of therapy) had significantly earlier onset activation of key virulence regulons and structural genes (eg, *sigB*, *sarA*, *sae*, and *cap5*), higher expression of purine biosynthesis genes (eg, *purF*), and faster growth rates, with earlier entrance into stationary phase. Importantly, an isogenic strain set featuring a wild-type MRSA isolate, a *purF* mutant strain, and a *purF*-complemented strain and use of strategic purine biosynthesis inhibitors implicated a causal relationship between purine biosynthesis and the in vivo persistent outcomes. These observations suggest that purine biosynthesis plays a key role in the outcome of PB and may represent a new target for enhanced efficacy in treating life-threatening MRSA infections.

Keywords. MRSA; purine biosynthesis; and persistent endovascular infection.

Staphylococcus aureus is a leading cause of life-threatening endovascular infections, including bacteremia and infective endocarditis [1, 2]. Despite the use of criterion-standard anti–methicillin-resistant *S. aureus* (MRSA) antibiotics (ie, vancomycin [VAN] and daptomycin [DAP]), treatment failures associated with these syndromes remain unacceptably high [3, 4]. Persistent bacteremia (PB), defined as bacteremia involving positive results of blood cultures for ≥7 days despite use of appropriate antibiotic therapy [3, 4], is an especially worrisome subset (proportion, 15%–30%) of these infections [5]. A key concern is that PB strains are usually deemed susceptible in vitro to VAN and DAP on the basis of CLSI breakpoints, yet they persist in vivo despite use of seemingly appropriate antibiotic therapy [3, 6]. Therefore, PB outcomes represent a unique and important variant of classic antibiotic resistance [7] and underscore an urgent need to understand the specific mechanism(s) of this syndrome.

De novo purine biosynthesis is a major pillar of nucleotide metabolism [8]. The purine biosynthesis pathway leads to the conversion of 5-phosphoribosyl-1-pyrophosphate to inosine monophosphate [9]. Among the purine synthesis pathway enzymes, amidophosphoribosyltransferase, encoded by *purF*, is a rate-limiting enzyme [8, 10]. The branch-point intermediate, inosine monophosphate, is the precursor to generation of 2 essential nucleobases, adenine and guanine, which serve as biosynthetic precursors for polymerizing reactions that generate DNA and RNA and as potential energy carriers [8, 11]. Therefore, the purine biosynthesis pathway is crucial for cell growth via DNA and RNA synthesis [10, 12]. Prior studies have reported that purine biosynthesis is involved in bacterial survival and virulence [10, 12, 13]. However, to our knowledge, the connection between purine biosynthesis and in vivo persistence of MRSA endovascular infections has not been described. Thus, the current investigation was designed to study the role of purine biosynthesis in PB outcomes, focusing on endovascular infections.

METHODS

Bacterial Strains

The study MRSA strains were from a multinational clinical trial collection and other sources, with the most common clonal complexes (CCs; eg, CC5, CC8, CC30, and CC45) and *agr* types (eg, *agr* I, II, and III) in circulation today causing clinical infections (Supplementary Table 1) [3, 4, 14–16]. The patients in the PB cohort and resolving bacteremia (RB) cohorts (defined as patients with positive results of initial MRSA blood cultures and negative results of subsequent blood cultures for 2–4 days after initiation of antibiotic therapy) were matched for demographic, epidemiologic, and clinical features (eg, age and underlying diseases) but differed significantly with respect to clinical outcome [3, 4,

Received 14 February 2018; editorial decision 29 May 2018; accepted 1 June 2018; published online June 2, 2018.

Correspondence: Y. Q. Xiong, MD, PhD, Los Angeles Biomedical Research Institute at Harbor-UCLA Medical Center, 1124 W Carson St, Torrance, CA 90502 (yxiong@ucla.edu).

The Journal of Infectious Diseases® 2018;218:1367–77

DOI: 10.1093/infdis/jiy340

14–16]. In addition, the selection of the study PB and RB strains was based on their CC types, *agr RNAIII* activation profiles, and response to VAN treatment in the infective endocarditis model, as reported previously [14, 15]. Importantly, all MRSA isolates that are considered susceptible to VAN on the basis of CLSI breakpoints have neither VAN in vitro tolerance nor VAN hetero-resistant subpopulations [3, 14–16]. JE2 and its *pur* mutant strains were from the Nebraska Transposon Mutant Library. The *purF* mutant was complemented with plasmid pSK236::*purF* [17].

Determination of VAN Minimum Inhibitory Concentrations (MICs)

MICs of VAN for JE2 parental and its *pur* mutant strains were determined by a standard Etest (BioMerieux, LABalmeles-Grottes, France), according to the manufacturer's recommended protocols.

Determination of Global Regulator/Gene Activation by Flow Cytometry

Several key global regulator/gene promoters relevant to the pathogenesis of *S. aureus*, including *asp23* (a surrogate for *sigB* activation), *sarA*, *sae*, and *cap5*, were cloned upstream of gfp_{uvr} in pALC1484 [18, 19]. Importantly, all study MRSA stains had *cap5* detected by PCR analysis (data not shown). MRSA stains cultured overnight and harboring plasmids P*asp23*::gfp_{uvr}, P*sarA*::gfp_{uvr}, P*sae*::gfp_{uvr}, or P*cap5*::gfp_{uvr} were diluted 1:100 into fresh tryptic soy broth (TSB) with or without the purine biosynthesis inhibitor 6-thioguanine (6-TG; 10 μg/mL) or mycophenolic acid (MPA; 50 μg/mL) and cultured at 37°C with shaking (200 rpm) for 24 hours. The concentrations of 6-TG and MPA used in these studies correspond to their pharmacokinetic profiles (eg, maximum concentration) in human recommended clinical dose [20, 21]. Samples were obtained hourly from 0 to 7 hours and then at 24 hours, to assess the profile of genes' promoter activation by flow cytometry [18].

Growth Curves and Generation Time

MRSA cells cultured overnight were suspended in phosphate-buffered saline to a density of 1.0 McFarland standard and diluted 1:100 into 50 mL of fresh TSB with or without the inhibitor 6-TG or MPA (at the same concentrations as described above) in 500-mL Erlenmeyer flasks. Samples were incubated at 37°C with shaking at 200 rpm, and cell growth was monitored spectrophotometrically hourly from 0 to 8 hours and then at 24 hours [22]. The generation time during the exponential phase was calculated from the data of growth curves [23].

Adenosine Triphosphate (ATP) and Adenosine Diphosphate (ADP) Levels

ATP and ADP levels in late-exponential cultures (incubated for 6 hours, corresponding the first time point that PB strains showed significantly higher *cap5* activation vs RB strains) were quantified by using the Promega BacTiter Glo kit and Promega ADP-Glo Kinase kit (Promega, Madison, WI), respectively [24, 25]. ATP and ADP levels were determined by measuring luminescence levels and comparing them to ATP and ADP standard curves, respectively, and are presented as concentrations normalized to the number of colony-forming units (CFU).

In Vitro VAN Killing Assay

To mimic in vivo conditions, a starting inoculum of 10^8 CFU/mL (comparable to MRSA counts in cardiac vegetation in the infective endocarditis model) of MRSA cells incubated for the same time (6 hours) as in the ATP and ADP assays described above was used for the VAN killing assay [14]. Surviving bacterial colony counts were determined after exposure to 15 μg/mL VAN (to mimic the targeted trough serum VAN concentration for severe MRSA infections in human) in cation-adjusted Mueller-Hinton broth for 24 hours [14, 16]. Survival rates were calculated as the number of surviving cells divided by the number of cells in the initial inoculum, multiplied by 100.

Microarray Analysis and Quantitative Reverse Transcription (qRT)–PCR Validation

A complementary DNA microarray was used to detect gene expression in prototype PB (300-169) and RB (301-188) strains after incubation for 3 hours (a time point related to the early onset activation of global regulators/genes) [26, 27]. The relative expression of *purF*, *purM*, and *purN* was confirmed by qRT-PCR [15, 28]. The level of *gyrB* expression was used to normalize transcript levels, and relative expression was calculated by the $\Delta\Delta C_T$ method [14].

Determination of 5-Aminoimidazole-4-Carboxamide Ribonucleotide (AICAR) Levels

To confirm the deficiency of purine biosynthesis in *pur* mutants, we tested the levels of AICAR (a purine biosynthetic intermediate) in the JE2 strain set. AICAR concentrations were detected by an enzyme-linked immunosorbent assay (MYBioSource, San Diego, CA) and are presented as the concentrations normalized to CFU.

Experimental Infective Endocarditis Model in Rabbits

To validate the in vivo role of purine biosynthesis in persistent MRSA outcomes, a well-characterized catheter-induced aortic valve infective endocarditis model in rabbits was used [29, 30]. In parallel experiments, 72 hours after catheterization, animals were infected intravenously with either the JE2 parental strain, its *purF* mutant, or its *purF*-complemented strain or with a representative PB strain (300-169) at the 95% infective dose previously established [28].

At 24 hours after infection with the JE2 strain set, animals were randomized into 1 of the following 8 groups (6–8 rabbits/group): (1) a group infected with the JE2 parental control strain, (2) a group infected with the JE2 parental control strain and treated intravenously twice daily with VAN at 7.5 mg/kg [28], (3) a group infected with the JE2 Δ*purF* control strain, (4) a group infected with the JE2 Δ*purF* strain and treated with VAN, (5) a group infected with the JE2 Δ*purF*/p*purF* control strain, (6) a group infected with the JE2 Δ*purF*/p*purF* strain and treated

with VAN, (7) a group infected with the JE2 parental strain and treated intraperitoneally twice daily with the purine biosynthesis inhibitor mycophenolate mofetil (MMF; a prodrug of MPA that confers improved bioavailability of MPA) at 80 mg/kg [31, 32], or (8) a group infected with the JE2 parental strain and treated with VAN and MMF.

For the PB strain (300-169), 24 hours after infection rabbits were randomized into 1 of the following 4 groups: (1) a group infected with a PB control strain, (2) a group infected with the PB strain and treated intravenously twice daily with VAN at 15 mg/kg [28], (3) a group infected with the PB strain and treated intraperitoneally twice daily with MMF at 80 mg/kg, or (4) a group infected with the PB strain and treated with VAN + MMF.

Treatments were given for 3 days. Twenty-four hours after the last treatment, the animals were euthanized. The cardiac vegetations, kidneys, and spleen were removed and quantitatively cultured individually for each animal [28, 30]. The mean $\log_{10}$ CFU/g of tissue (±SD) was calculated for each target tissue for statistical comparisons. The Institutional Animal Care and Use Committee of the Los Angeles Biomedical Research Institute at Harbor-UCLA Medical Center approved all animal studies.

Statistical Analysis

All in vitro experiments were performed in triplicate with at least 2 biological replicates. A 2-tailed Student *t* test was used to analyze the in vitro data and tissue MRSA counts between

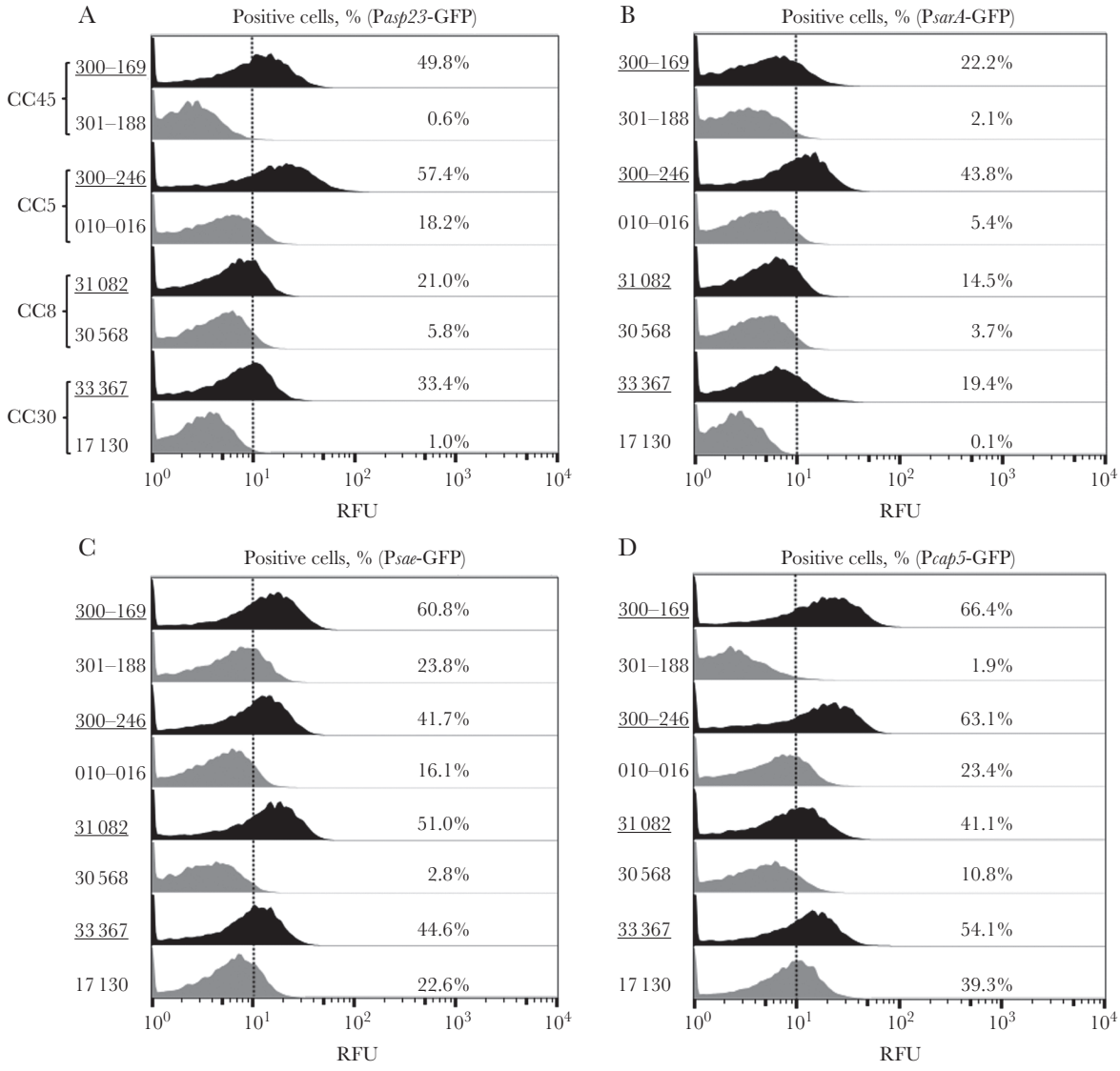

Figure 1. Expression of *asp23* (*A*), *sarA* (*B*), *sae* (*C*), and *cap5* (*D*) in clinical persistent methicillin-resistant *Staphylococcus aureus* (MRSA) bacteremia (PB) strains (underlined) and resolving MRSA bacteremia (RB) strains after incubation for 6 hours by flow cytometry. Relative fluorescence units (RFU) were used to measure green fluorescent protein (GFP) expression. Cells with >10 RFU were demonstrated as positive for GFP expression. The percentage of GFP-positive cells from each group was analyzed. The results are representative of flow cytometry data in histograms from 1 replicate.

different groups. Data were expressed as mean (±SD). *P* values <.05 were considered significant. No adjustment was made for *P* values reported in this study.

RESULTS

PB Strains Exhibited Significantly Earlier Activation of Key Global Regulators/Structural Genes and Faster Growth Than RB Strains

We found that, as compared to RB strains, PB strains exhibited a relatively earlier transcriptional onset of several key regulatory and structural genes involved in MRSA virulence, as measured by increased green fluorescent protein expression in their promoters (Figure 1 and Supplementary Table 2). For instance, after incubation for 6 hours (corresponding to the first time point that showed significantly different gene activation levels between all PB and RB strains), the percentage of cells exhibiting *asp23* promoter activation (as a surrogate for *sigB* activation) in PB strain 300-169 was approximately 50%, compared with <1% in RB strain 301-188 (Figure 1A). Of note, all PB strains exhibited earlier activation and higher expression of *cap5* than RB strains (Figure 1D and Supplementary Table 2). Since *cap5* is specifically activated in the stationary phase [33], we hypothesized that PB strains may be entering the stationary phase earlier than RB strains. Supporting our hypothesis, the growth curve revealed that PB strains had significantly faster growth rates and shorter generation times than RB strains ($P < .05$; Figure 2).

PB Strains Demonstrated Significantly Higher Purine Biosynthesis Gene Expression Than RB Strains

Microarray analyses revealed an increased (by ≥2-fold) transcription of 78 distinct genes, with a concomitant decrease in expression of 61 other genes in PB strain 300-169, compared with RB strain 301-188 (Figure 3A and 3B, respectively). In addition to the expected global regulators, the transcription of multiple purine biosynthesis genes (eg, *purF*, *purM*, and *purN*) was significantly higher in the PB strain, compared with the RB strain. These microarray results were verified by qRT-PCR assays ($P < .01$; Figure 3C). In addition, the expression of *purF*, *purM*, and *purN* were also confirmed to be significantly upregulated in all study PB strains, compared with the RB strains ($P < .01$; Supplementary Figure 1).

Disruption of the Purine Biosynthesis Pathway Converted PB Strains to RB-Like Phenotypes

To test the hypothesis that purine biosynthesis is integral to PB outcomes, a parental MRSA strain, JE2, and its *purF*, *purM*, and *purN* mutants were examined [34]. First, we validated that purine biosynthesis was indeed deficient in each of the individual *pur* mutants by measuring levels of AICAR

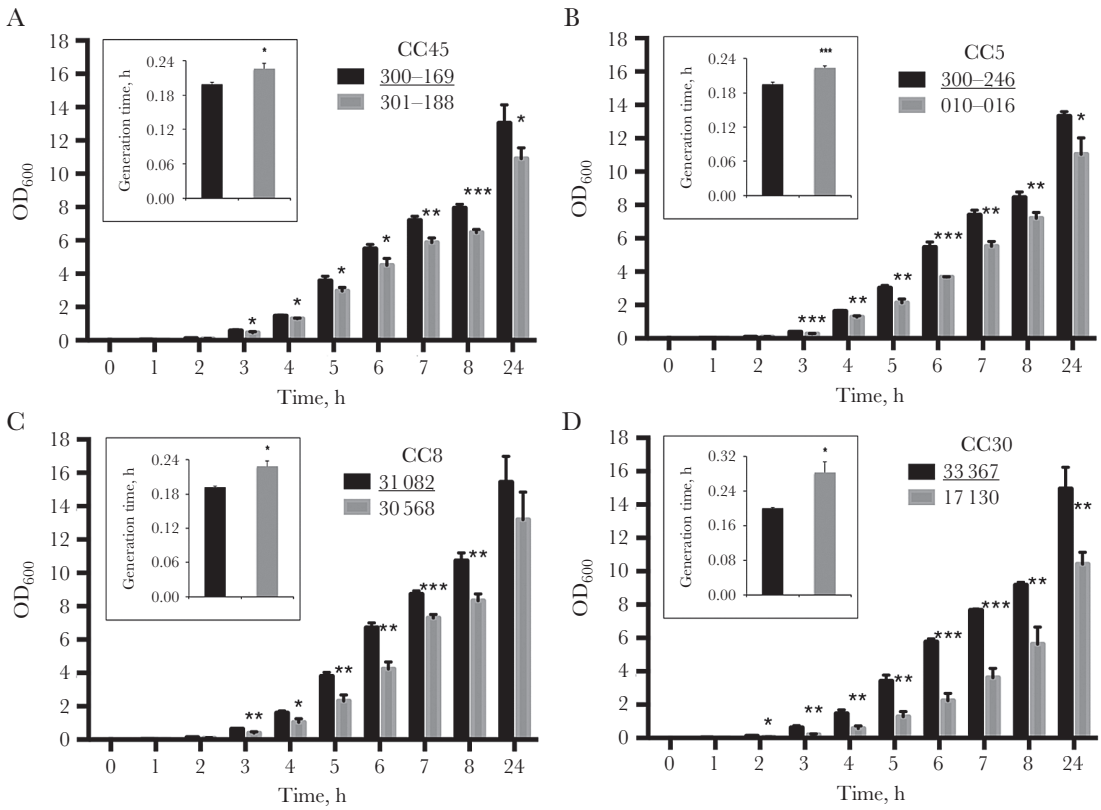

Figure 2. Growth curves and generation times (inset; during exponential phase) of persistent methicillin-resistant *Staphylococcus aureus* (MRSA) bacteremia (PB) strains (black, underlined) and resolving MRSA bacteremia (RB) strains (gray). **P* < .05, ***P* < .01, and ****P* < .001, compared with PB strains.

($P < .05$; Supplementary Figure 2*A*). Importantly, similar to the clinical RB strains, each of these mutants showed significantly (1) slower growth rates and longer generation times ($P < .05$; Supplementary Figure 2*B*); and (2) later-onset activation of *asp23*, *sarA*, *sae*, and *cap5*, compared with their JE2 parental strain (Supplementary Figure 2*C* and Table 3; data are shown for the *purF* mutant but not for the *purM* and *purN* mutants).

Importantly, *purF* complementation confirmed the impact of *purF* on purine biosynthesis ($P < .001$; Figure 4A) and showed higher *purF* expression ($P < .0001$; Figure 4B) than the parental strain, consistent with the high-copy-number plasmid used for the *purF* complementation (pSK236, approximately 15 copies) [18]. Interestingly, the growth rate and generation time phenotypes of the *purF*-complemented strain were only partially restored to those of the parental strain ($P < .05$; Figure 4C). These latter findings may be associated with a probable fitness cost of the multicopy plasmid.

Lower ATP Levels at the Late-Exponential Phase Correlated With Higher Survival With VAN Exposure in the PB Strain Versus the RB Strain and the JE2 Parental Strain Versus Its Isogenic purF Mutant

We demonstrated that PB cells in the late-exponential phase (ie, after incubation for 6 hour) exhibited significantly lower ATP levels ($P < .01$; Figure 5A), paralleling a higher survival rate with VAN exposure, compared with RB strains ($P < .05$ [Figure 5B] and $P < .01$ [Supplementary Figure 4*A*]). Interestingly, a similar relationship between ATP levels and survival with VAN exposure was observed in the JE2 strain set ($P < .01$; Figure 5C and 5D and Supplementary Figure 4*B*). In addition, significantly higher ADP levels were seen in JE2 parental and *purF*-complemented strains as compared to the *purF* mutant at the same time point ($P < .001$; Figure 5C). These results indicate that the JE2 parental strain might have a higher synthesized ATP level at this time point. The decreased intracellular ATP levels in the PB and JE2 parental strains may link to their faster growth and earlier entrance into the stationary phase.

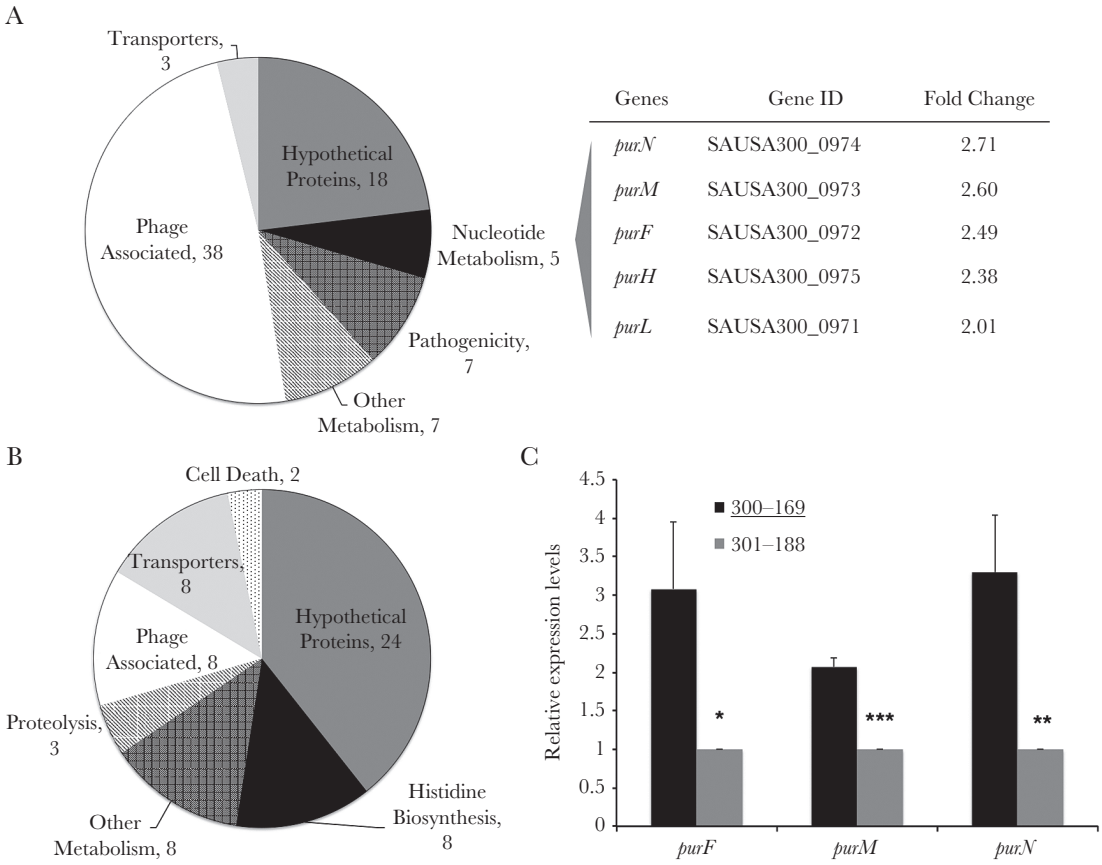

Figure 3. *A* and *B*, Distribution of upregulated (*A*) and downregulated (*B*) genes in a representative persistent methicillin-resistant *Staphylococcus aureus* (MRSA) bacteremia (PB) strain (300-169) versus a resolving MRSA bacteremia (RB) strain (301-188) as determined by microarray analysis after incubation for 3 hours. *C*, Confirmation of *purF*, *purM*, and *purN* expression in the PB strain (300-169; black, underlined) versus the RB stain (301-188; gray) as determined by quantitative reverse transcription polymerase chain reaction analysis. Primers used were as follows: *purF*, 5′-CGTGAGCAAGGTGTGAGAGT-3′ and 5′-CGAATTGTCGTACCGCGAAC-3′; *purM*, 5′-AACGACAGGTGCAGAACCAT-3′ and 5′-TTTCAGCAGTCTCTCCACCG-3′; and *purN*, 5′-AGCTGGCTACATGCGTCTAA-3′ and 5′-GCCTATTGCGTCAATCCCCT-3′. *$P < .01$, **$P < .001$, and ***$P < .0001$, compared with PB strain 300-169.

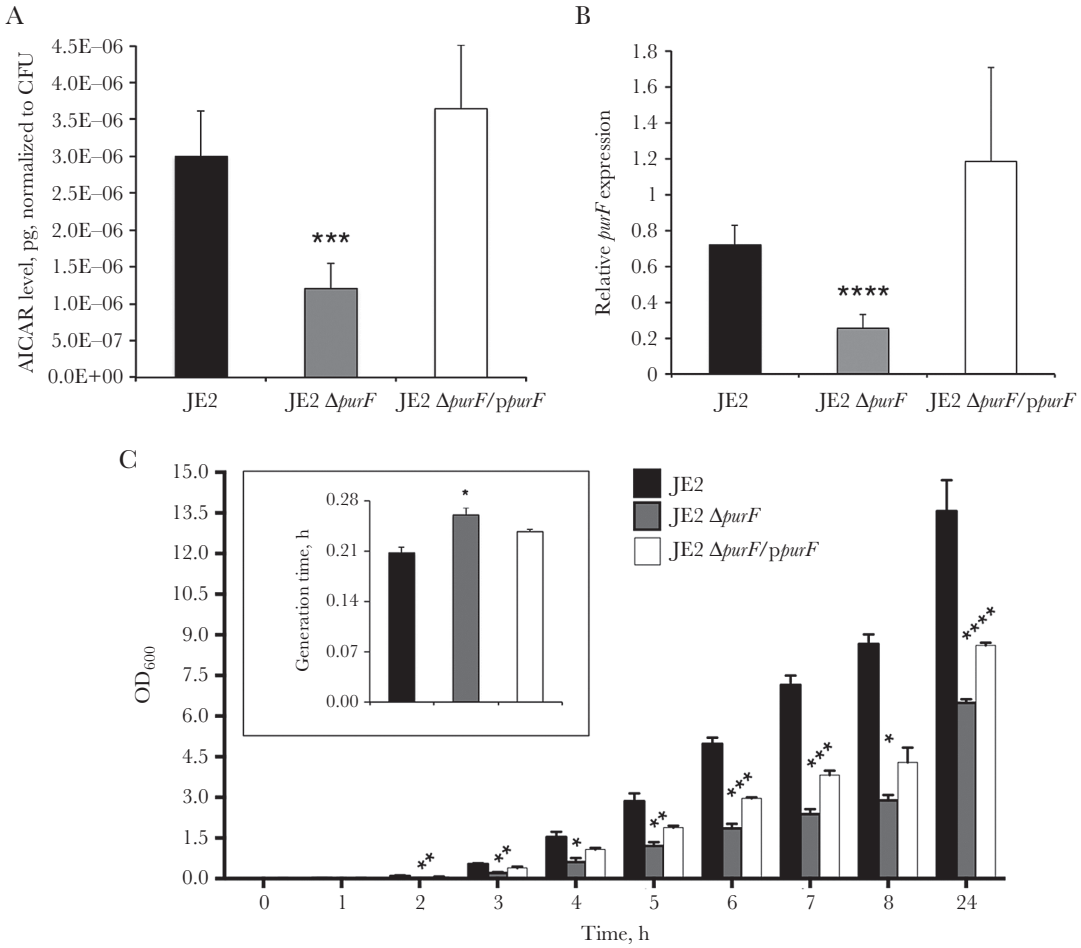

Figure 4. *A* and *B*, 5-Aminoimidazole-4-carboxamide ribonucleotide (AICAR) levels (*A*) and relative expression of *purF* (*B*) after incubation for 3 hours in the JE2 parental strain, and its *purF*-mutant and *purF*-complemented strains. *C*, Growth curves and generation times (inset) in the JE2 parental strain and its isogenic *purF*-mutant and *purF*-complemented strains. **P* < .05, ***P* < .01, ****P* < .001, and *****P* < .0001, compared with the JE2 parental and *purF*-complemented strains.

Purine Biosynthesis Inhibition Converted the JE2 Parental Strain to RB-Like Phenotypes

Similar to data seen in the *pur* mutant and clinical RB strains above, a slower growth, longer generation time, later-onset activation of global regulators/structural genes, higher ATP levels, and lower survival after VAN exposure were observed in the 6-TG– or MPA-treated parental JE2 strain ($P < .01$; Supplementary Figure 3).

Purine Biosynthesis Profiles Correlated With Persistent Outcomes in an Experimental MRSA Infective Endocarditis Model

To translate the putative impact of purine biosynthesis in the outcome of PB in vivo, an experimental infective endocarditis model was used. The *purF* mutant had slightly lower MRSA counts in the target tissues than its parental JE2 strain (Figure 6A). However, these differences did not reach statistical significance. Interestingly, the *purF* mutant–infected animals were hypersusceptible to VAN treatment, with all target tissues being sterilized, compared with untreated *purF* mutant controls or animals infected with the JE2 parental strain, with or without VAN treatment ($P < .05$; Figure 6A). Also, it is notable that the *purF*-complemented variant was resistant to VAN treatment, with significantly higher MRSA densities in the target tissues as compared to VAN-treated animals infected with the JE2 parental strain ($P < .05$; Figure 6A). Importantly, in animals infected with PB strain 300-169, VAN treatment did not yield any significant reductions of MRSA densities in any target tissues (Figure 6B), which is consistent with the PB outcome in clinical settings.

Notably, treatment with the purine biosynthesis inhibitor MMF alone had no effect in reducing MRSA densities in any target tissues as compared to untreated controls (Figure 6A and 6B for JE2 and 300-169 strains, respectively). However, the combination treatment of VAN and MMF yielded significant reductions of target tissue MRSA densities in animals infected with the JE2 parental (except spleen) or PB 300-169 strains, compared with VAN treatment alone ($P < .05$; Figure 6A and 6B).

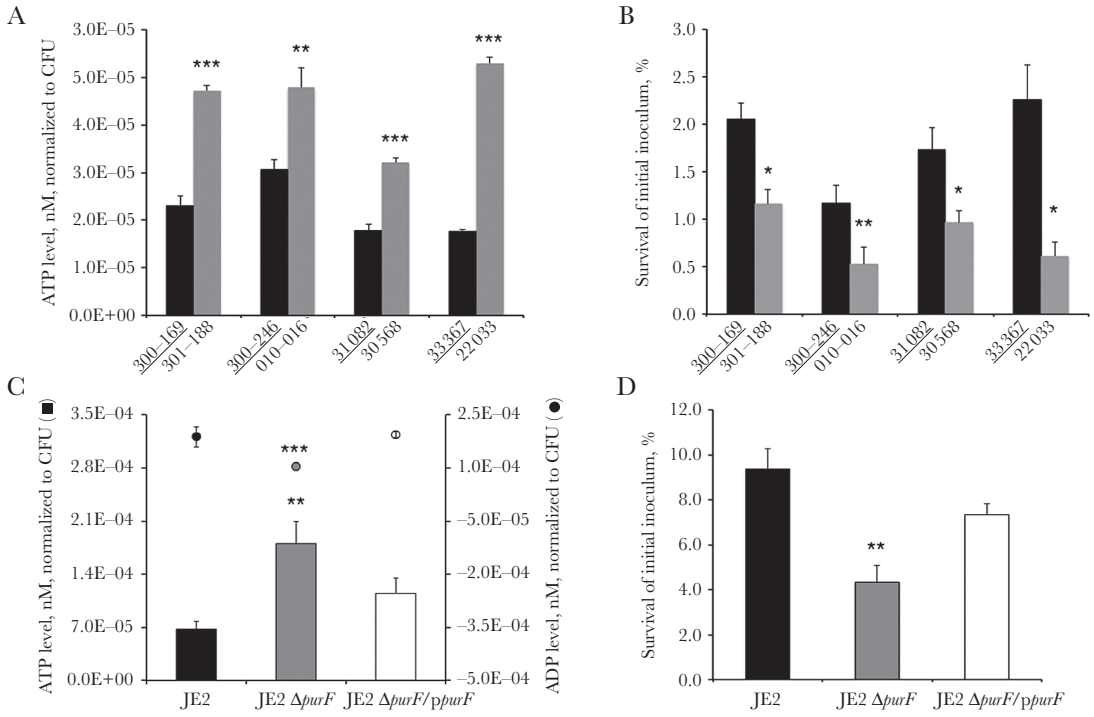

Figure 5. *A* and *B*, Adenosine triphosphate (ATP) levels (*A*) and survival rates after vancomycin (VAN) exposure (15 µg/mL for 24 hours; *B*) among persistent methicillin-resistant *Staphylococcus aureus* (MRSA) bacteremia (PB) strains (black, underlined) and resolving MRSA bacteremia (RB) strains (gray) at the late-exponential phase (ie, after incubation for 6 hours; starting inoculum, 10^8 colony-forming units [CFU]/mL). *C* and *D*, ATP and adenosine diphosphate (ADP) levels (*C*) and survival rates after VAN exposure (15 µg/mL for 24 hours; *D*) among the JE2 parental strain and its *purF*-mutant and *purF*-complemented strains after incubation for 6 hours (ie, during the late-exponential phase; starting inoculum, 10^8 CFU/mL). **P* < .05, ***P* < .01, and ****P* < .001, compared with their respective PB strains (*A* and *B*) and the JE2 parental and *purF*-complemented strains (*C* and *D*).

DISCUSSION

A number of interesting observations emerged from our current studies, especially the relationship between purine biosynthesis and PB outcomes. First, our transcriptional profiling experiments revealed a significantly higher expression of purine biosynthesis pathway genes in clinical PB strains versus RB strains. Previous studies have shown that purine biosynthesis contributes importantly to DNA replication and RNA production to support protein synthesis and subsequently influence bacterial growth, as well as bacterial intracellular survival and virulence of pathogens [12, 13]. Second, we demonstrated that PB strains exhibited significantly earlier-onset activation of a number of key global regulators as compared to RB strains. These global regulators were selected because they have each been shown to influence transcription of key virulence genes and antimicrobial susceptibility in vivo, including infective endocarditis [30, 35, 36]. The current transcriptional data are also concordant with data from other studies showing that purine biosynthesis profoundly affects the activation of global regulators in *S. aureus* (eg, *sigB* and *sae*) [13]. Third, significantly earlier *cap5* expression was demonstrated in PB strains versus RB strains. These results suggested that PB strains reach the stationary phase earlier than RB strains. Growth kinetics confirmed the significantly faster growth rates and shorter generation times in PB strains versus RB strains. Accordingly, similar to the RB strains, a *purF* mutant strain showed slower growth rates and later-onset activation of global regulators, compared with its isogenic JE2 parental strain. Taken together, these results suggest a correlation among purine biosynthesis, growth kinetics, and temporal activation of key global regulators in MRSA strains.

Persistent infections caused by *S. aureus* have been associated with evolution of persisters and/or small-colony variant (SCV) phenotypes. Persisters compose a subpopulation of bacteria that become tolerant to bactericidal antibiotics [33]. The mechanism(s) for the formation of persisters are related to a number of factors, including the toxin-antitoxin system and the general stress response [37]. In contrast, SCVs are typically characterized by a slow-growth phenotype due to several pathogenic pathway alterations to protect *S. aureus* from the bactericidal activity of many antibiotics [37, 38]. This raised the question of whether the PB strains in our investigation represented either persisters and/or SCVs. Multiple lines of evidence argued against these possibilities. First, our PB isolates had neither VAN tolerance [14, 15] nor typical SCV colonial morphology (ie, minute colonies without pigmentation or hemolysis; data not shown). In addition, our study PB strains exhibited

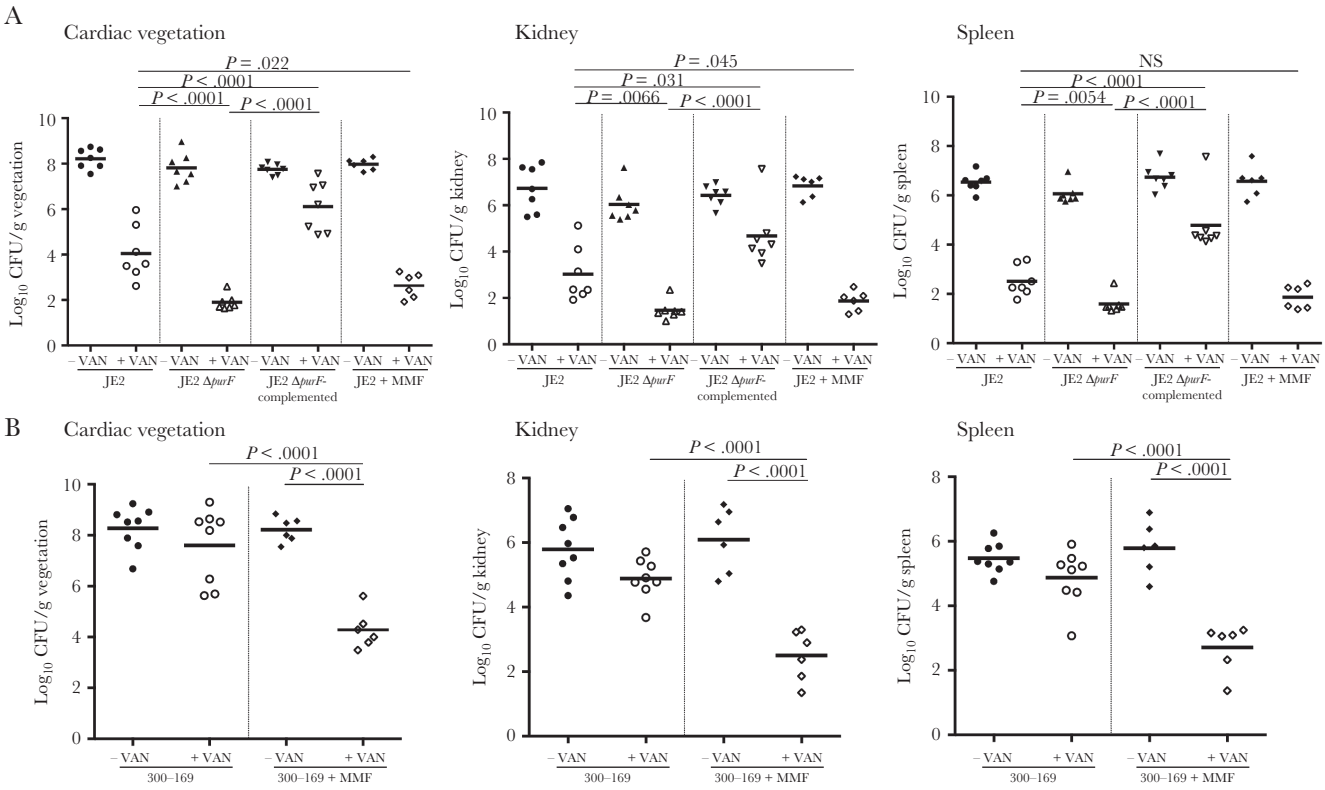

Figure 6. Densities of methicillin-resistant *Staphylococcus aureus* (MRSA) in target tissues in the infective endocarditis model after challenge with 10^5 colony-forming units of study MRSA isolates (*A*, JE2 strain set; *B*, strain 300-169) with and without vancomycin (VAN) or mycophenolate mofetil (MMF) treatment. Each dot represents 1 animal. Horizontal black bars indicate mean MRSA densities. NS, not significant.

significantly faster growth rates than the RB strains. Similar to our findings, Richard et al demonstrated faster growth rates in PB strains, compared with RB strains, under nutrient-poor conditions [39]. Taken together, our PB isolates represent a novel mechanism of persistence.

Certain nutrients, such as carbon source molecules (eg, glucose) and amino acid molecules (eg, glutamine), are necessary to initiate de novo purine biosynthesis [40]. Therefore, the nucleotide pools, including ATP, begin to decrease when bacterial cells reach stationary phase or even mid-exponential phase, owing to nutrient limitation [41]. Consistently, the observed increase in growth rates of our PB strains suggests the possibility of at least 2 relationships with PB outcomes: (1) a greater ratio of MRSA subpopulations of heterogenic stationary-phase cells emerging in the exponential phase would be reflected by significantly lower ATP levels in PB strains, compared with RB strains; and/or (2) purine biosynthesis itself would consume ATP, reflecting lower intracellular ATP levels [10, 40]. In addition, a decline in ATP levels could decrease the activity of ATP-consuming antibiotic targets, leading to reduced antibiotic killing activity [33, 42]. In the current studies, we also examined the ability of VAN to kill late-exponential/early stationary-phase PB cells versus RB cells. These experiments showed that decreased ATP levels in PB strains versus RB strains were associated with significantly higher survival upon VAN exposures (despite both PB and RB strains having similar VAN MICs) [14, 15]. These findings are consistent to those of Conlon et al, who recently reported that increased *S. aureus* survival rates after exposure to several antibiotics, including VAN, occurred in the stationary phase of growth [33]. It is known that VAN binds directly to D-alanyl-D-alanine and prevents subsequent cross-linking by transpeptidase, thus inhibiting bacterial cell wall synthesis. Because ATP is needed to drive D-alanyl-D-alanine synthesis, lower ATP levels could result in reduced binding of VAN to D-alanyl-D-alanine and, subsequently, reduced VAN bactericidal activity [42]. In this regard, the fast-growth phenotype in PB strains leading to lower intracellular ATP levels at the late-exponential to stationary phase of growth might provide a distinct survival advantage in the presence antibiotic exposure.

Our isogenic strain set featuring wild-type MRSA JE2, its isogenic *purF* mutant, and *purF*-complemented variants validated the relationship among purine biosynthesis, growth rate, ATP levels, and VAN susceptibility.

Notably, the in vitro genotypic and phenotypic findings outlined above were translatable into significant outcome differences in experimental infective endocarditis. Of great importance, animals infected with the *purF* mutant were hypersusceptible to VAN treatment. These outcomes may be due at

least to in part a combination of deficient purine biosynthesis and subsequent enhanced susceptibility to VAN-mediated killing. In addition, differential timing of the activation of global regulons/genes may also influence VAN treatment outcomes in MRSA infection. It has been reported that *sigB* plays a crucial function in promoting bacterial intracellular persistence via defending *S. aureus* from invading immune cells [23]. In addition, *sarA* plays an important role in biofilm formation, within which the organisms become more resistant to antibiotics and host defense effectors [28]. Interestingly, the *purF*-complemented variant was more resistant to VAN treatment than its parental JE2 strain in the infective endocarditis model. This outcome may be related to the high-copy-number plasmid used for *purF* complementation, which may drive excess purine biosynthesis [18].

Purine biosynthesis inhibitors, such as 6-TG and MPA, inhibit enzymes in the purine biosynthesis pathway (Figure 7) [13, 43]. In agreement with our data on the purine biosynthesis knockout mutants, we demonstrated that 6-TG or MPA exposure significantly decreased growth rates and led to delayed activation of global regulators/genes in the JE2 parental strain. Further, addition of MMF, a prodrug of MPA, significantly enhanced VAN treatment efficacy in the infective endocarditis model, compared with the efficacy of either drug alone against the JE2 or 300-169 strains. This finding is compelling evidence that purine biosynthesis plays a key role in the persistence outcome. Both 6-TG and MPA have been used clinically for many years for patients with certain leukemias and organ transplantation, respectively. Their major well-known adverse effects include perturbations of immune function, especially bone marrow suppression. The existence of such side effects may suggest that the use of such agents in antiinfective therapy is counterintuitive. In this regard, the current in vivo studies using MMF should be considered as initial proofs of concept that modulation of purine metabolism in MRSA may have beneficial net effects on outcomes in endovascular infection. It should also be emphasized that any potential use of such inhibitors for antimicrobial purposes would only be for short-term strategies (as opposed to long-term use in leukemia or organ transplantation regimens).

With the current rising threat of MRSA persistence, development of a new therapeutic strategy that can mitigate the activation of bacterial virulence genes related to PB is considered a high priority. In this respect, targeting purine biosynthesis may have the potential to be an effective adjunctive treatment against life-threatening PB.

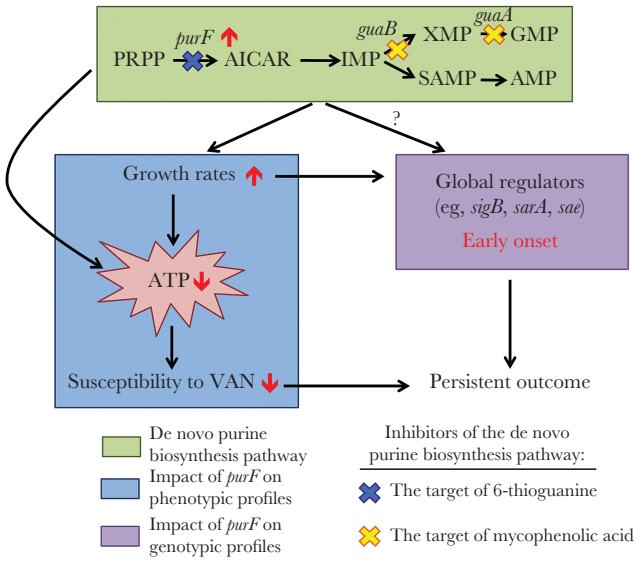

Figure 7. Hypothesized model of the role of purine biosynthesis in the outcome of persistent methicillin-resistant *Staphylococcus aureus* (MRSA) bacteremia. De novo purine biosynthesis pathway mediates the conversion of 5-phosphoribosyl-1-pyrophosphate (PRPP) to inosine monophosphate [8], which subsequently become the purines adenosine monophosphate (AMP) and guanosine monophosphate (GMP). The elevated transcription of *purF*, encoding the rate-limit enzyme amidophosphoribosyltransferase (PRPP→PRA), in the purine biosynthesis pathway leads to (1) an increased growth rate, (2) early-onset activation of global regulators, and (3) decreased adenosine triphosphate (ATP) levels in MRSA strains. Reduction in ATP levels promotes MRSA survival with vancomycin (VAN) exposure, which, in addition to the early onset activation of global regulators, contributes to the persistent outcomes in MRSA endovascular infection. 6-Thioguanine and mycophenolic acid inhibit enzymes in the purine biosynthesis pathway, including ATPase, inosine monophosphate (IMP) dehydrogenase (produced by *guaB*; IMP→XMP), and GMP synthetase (produced by *guaA*; XMP→GMP).

Supplementary Data

Supplementary materials are available at *The Journal of Infectious Diseases* online. Consisting of data provided by the authors to benefit the reader, the posted materials are not copyedited and are the sole responsibility of the authors, so questions or comments should be addressed to the corresponding author.

Notes

Financial support. This work was supported by the National Institutes of Health (grants AI-097657 [to Y. Q. X.], AI-091801 [to A. L. C.], AI-039108 [to A. S. B.], and AI-124319 and AI-111661 [to M. R. Y.]) and South China Agricultural University (scholarship to Y.-F. Z.).

Potential conflicts of interest. M. R. Y. is a founder of NovaDigm Therapeutics, which focuses on antiinfective vaccines and immunotherapeutics, including those targeting *Staphylococcus aureus* and MRSA. All other authors report no potential conflicts of interest. All authors have submitted the ICMJE Form for Disclosure of Potential Conflicts of Interest.

References

1. Klevens RM, Morrison MA, Nadle J, et al. Invasive methicillin-resistant *Staphylococcus aureus* infections in the United States. JAMA **2007**; 298:1763–71.
2. Fowler VG Jr, Miro JM, Hoen B, et al.; ICE Investigators. *Staphylococcus aureus* endocarditis: a consequence of medical progress. JAMA **2005**; 293:3012–21.

3. Fowler VG Jr, Sakoulas G, McIntyre LM, et al. Persistent bacteremia due to methicillin-resistant *Staphylococcus aureus* infection is associated with *agr* dysfunction and low-level in vitro resistance to thrombin-induced platelet microbicidal protein. J Infect Dis **2004**; 190:1140–9.
4. Xiong YQ, Fowler VG, Yeaman MR, Perdreau-Remington F, Kreiswirth BN, Bayer AS. Phenotypic and genotypic characteristics of persistent methicillin-resistant *Staphylococcus aureus* bacteremia in vitro and in an experimental endocarditis model. J Infect Dis **2009**; 199:201–8.
5. Khatib R, Johnson LB, Fakih MG, et al. Persistence in *Staphylococcus aureus* bacteremia: incidence, characteristics of patients and outcome. Scand J Infect Dis **2006**; 38:7–14.
6. Seidl K, Bayer AS, Fowler VG Jr, et al. Combinatorial phenotypic signatures distinguish persistent from resolving methicillin-resistant *Staphylococcus aureus* bacteremia isolates. Antimicrob Agents Chemother **2011**; 55:575–82.
7. Conlon BP, Nakayasu ES, Fleck LE, et al. Activated ClpP kills persisters and eradicates a chronic biofilm infection. Nature **2013**; 503:365–70.
8. Kilstrup M, Hammer K, Ruhdal Jensen P, Martinussen J. Nucleotide metabolism and its control in lactic acid bacteria. FEMS Microbial Rev **2005**; 29:555–90.
9. Zhang Y, Morar M, Ealick SE. Structural biology of the purine biosynthetic pathway. Cell Mol Life Sci **2008**; 65:3699–724.
10. Yamaoka T, Kondo M, Honda S, et al. Amidophosphoribosyltransferase limits the rate of cell growth-linked de novo purine biosynthesis in the presence of constant capacity of salvage purine biosynthesis. J Biol Chem **1997**; 272:17719–25.
11. Voet DV, Pratt C. Fundamentals of biochemistry: life at the molecular level. 3rd ed. Hoboken, NJ: Wiley, **2008**.
12. Samant S, Lee H, Ghassemi M, et al. Nucleotide biosynthesis is critical for growth of bacteria in human blood. PLoS Pathog **2008**; 4:e37.
13. Lan L CA, Dunman PM, Missiakas D, He C. Golden pigment production and virulence gene expression are affected by metabolisms in *Staphylococcus aureus*. J Bacteriol **2010**; 192:3068–77.
14. Seidl K, Chen L, Bayer AS, Hady WA, Kreiswirth BN, Xiong YQ. Relationship of *agr* expression and function with virulence and vancomycin treatment outcomes in experimental endocarditis due to methicillin-resistant *Staphylococcus aureus*. Antimicrob Agents Chemother **2011**; 55:5631–9.
15. Abdelhady W, Chen L, Bayer AS, et al. Early *agr* activation correlates with vancomycin treatment failure in multi-clonotype MRSA endovascular infections. J Antimicrob Chemother **2015**; 70:1443–52.
16. Abdelhady W, Bayer AS, Seidl K, et al. Reduced vancomycin susceptibility in an in vitro catheter-related biofilm model correlates with poor therapeutic outcomes in experimental endocarditis due to methicillin-resistant *Staphylococcus aureus*. Antimicrob Agents Chemother **2013**; 57:1447–54.
17. Manna AC, Ingavale SS, Maloney M, van Wamel W, Cheung AL. Identification of *sarV* (SA2062), a new transcriptional regulator, is repressed by SarA and MgrA (SA0641) and involved in the regulation of autolysis in *Staphylococcus aureus*. J Bacteriol **2004**; 186:5267–80.
18. Xiong YQ, Van Wamel W, Nast CC, Yeaman MR, Cheung AL, Bayer AS. Activation and transcriptional interaction between *agr RNAII* and *RNAIII* in *Staphylococcus aureus* in vitro and in an experimental endocarditis model. J Infect Dis **2002**; 186:668–77.
19. Heim R, Cubitt AB, Tsien RY. Improved green fluorescence. Nature **1995**; 373:663–4.
20. Lowe ES, Kitchen BJ, Erdmann G, et al. Plasma pharmacokinetics and cerebrospinal fluid penetration of thioguanine in children with acute lymphoblastic leukemia: a collaborative Pediatric Oncology Branch, NCI, and Children's Cancer Group study. Cancer Chemother Pharmacol **2001**; 47:199–205.
21. Bullingham R, Monroe S, Nicholls A, Hale M. Pharmacokinetics and bioavailability of mycophenolate mofetil in healthy subjects after single-dose oral and intravenous administration. J Clin Pharmacol **1996**; 36:315–24.
22. Somerville GA, Powers R. Growth and preparation of *Staphylococcus epidermidis* for NMR metabolomic analysis. Methods Mol Biol **2014**; 1106:71–91.
23. Tuchscherr L, Bischoff M, Lattar SM, et al. Sigma factor SigB is crucial to mediate *Staphylococcus aureus* adaptation during chronic infections. PLoS Pathog **2015**; 11:e1004870.
24. Mempin R, Tran H, Chen C, Gong H, Kim Ho K, Lu S. Release of extracellular ATP by bacteria during growth. BMC Microbiol **2013**; 13:301.
25. Zegzouti H, Zdanovskaia M, Hsiao K, Goueli SA. ADP-Glo: a bioluminescent and homogeneous ADP monitoring assay for kinases. Assay Drug Dev Technol **2009**; 7:560–72.
26. Koziel J, Maciag-Gudowska A, Mikolajczyk T, et al. Phagocytosis of *Staphylococcus aureus* by macrophages exerts cytoprotective effects manifested by the upregulation of antiapoptotic factors. PLoS One **2009**; 4:e5210.
27. Kobayashi SD, Braughton KR, Whitney AR, et al. Bacterial pathogens modulate an apoptosis differentiation program in human neutrophils. Proc Natl Acad Sci U S A **2003**; 100:10948–53.
28. Abdelhady W, Bayer AS, Seidl K, et al. Impact of vancomycin on *sarA*-mediated biofilm formation: role in persistent endovascular infections due to methicillin-resistant *Staphylococcus aureus*. J Infect Dis **2014**; 209:1231–40.
29. Seidl K, Bayer AS, McKinnell JA, Ellison S, Filler SG, Xiong YQ. In vitro endothelial cell damage is positively correlated with enhanced virulence and poor vancomycin responsiveness in experimental endocarditis due to

methicillin-resistant *Staphylococcus aureus*. Cell Microbiol **2011**; 13:1530–41.
30. Li L, Cheung A, Bayer AS, et al. The global regulon *sarA* regulates β-lactam antibiotic resistance in methicillin-resistant *Staphylococcus aureus* in vitro and in endovascular infections. J Infect Dis **2016**; 214:1421–9.
31. Yatscoff RW, Keenan R, LeGatt DF. Single-dose pharmacokinetics of the new immunosuppressant RS-61443 in the rabbit. Ther Drug Monit **1993**; 15:400–4.
32. Villarroel MC, Hidalgo M, Jimeno A. Mycophenolate mofetil: an update. Drugs Today (Barc) **2009**; 45:521–32.
33. Conlon BP, Rowe SE, Gandt AB, et al. Persister formation in *Staphylococcus aureus* is associated with ATP depletion. Nat Microbiol **2016**; 1:16051.
34. Fey PD, Endres JL, Yajjala VK, et al. A genetic resource for rapid and comprehensive phenotype screening of nonessential *Staphylococcus aureus* genes. MBio **2013**; 4:e00537–12.
35. Xiong YQ, Willard J, Yeaman MR, Cheung AL, Bayer AS. Regulation of *Staphylococcus aureus* alpha-toxin gene (*hla*) expression by *agr*, *sarA*, and *sae* in vitro and in experimental infective endocarditis. J Infect Dis **2006**; 194:1267–75.
36. Liu Q, Yeo WS, Bae T. The SaeRS two-component system of *Staphylococcus aureus*. Genes **2016**; 7:81.
37. Zhang Y. Persisters, persistent infections and the Yin-Yang model. Emerg Microbes Infect **2014**; 3:e3.
38. Proctor RA, Balwit JM, Vesga O. Variant subpopulations of *Staphylococcus aureus* as cause of persistent and recurrent infections. Infect Agents Dis **1994**; 3:302–12.
39. Richards RL, Haigh RD, Pascoe B, et al. Persistent *Staphylococcus aureus* isolates from two independent cases of bacteremia display increased bacterial fitness and novel immune evasion phenotypes. Infect Immun **2015**; 83:3311–24.
40. Schultheisz HL, Szymczyna BR, Scott LG, Williamson JR. Pathway engineered enzymatic de novo purine nucleotide synthesis. ACS Chem Biol **2008**; 3:499–511.
41. Buckstein MH, He J, Rubin H. Characterization of nucleotide pools as a function of physiological state in *Escherichia coli*. J Bacteriol **2008**; 190:718–26.
42. Kuzin AP, Sun T, Jorczak-Baillass J, Healy VL, Walsh CT, Knox JR. Enzymes of vancomycin resistance: the structure of D-alanine-D-lactate ligase of naturally resistant *Leuconostoc mesenteroides*. Structure **2000**; 8:463–70.
43. Christopherson RI, Lyons SD, Wilson PK. Inhibitors of de novo nucleotide biosynthesis as drugs. Acc Chem Res **2002**; 35:961–71.